

Optimizing mechanical properties of multi-walled carbon nanotube reinforced thermoplastic polyurethane composites for advanced athletic protective gear

Jing Su¹ 

¹Anhui Sport Vocational and Technical College, Department of Physical Education Management, Huayuan Avenue, Hefei, Anhui Province 230051, China.

e-mail: sojing88@sina.com

ABSTRACT

This study investigates the mechanical properties of thermoplastic polyurethane (TPU) composites reinforced with multi-walled carbon nanotubes (MWCNTs) for application in athletic protective gear. The objectives were to (1) systematically evaluate the effects of MWCNT loading level and alignment on the tensile, compressive, hardness, and impact properties; (2) identify an optimal MWCNT content range for balanced enhancements; and (3) explore scalable fabrication methods. MWCNT/TPU composites with 0.5–4 wt% loading were prepared by solution mixing and compression molding. Mechanical testing revealed significant improvements, with 62 MPa tensile strength (+19%), 507 MPa modulus (+23%), and 10% higher impact energy absorption achieved at 1–4 wt% MWCNT. MWCNT alignment further enhanced the properties, while loadings above 2 wt% showed some embrittlement. Microstructural characterization evidenced good MWCNT dispersion and interfacial bonding. The results demonstrate that low MWCNT additions can substantially enhance the strength, stiffness, and impact resistance of TPU. This indicates great potential for developing advanced, lightweight athletic protective equipment like helmets and pads with improved energy absorption and durability. Future work will focus on optimizing composite processing and design for specific gear applications.

Keywords: Composite Material; Impact Resistance; Tensile Strength; Nano-reinforcement; Polymer Matrix.

1. INTRODUCTION

Athletic protective gear is essential for preventing injuries in contact sports and high-impact activities. Helmets, pads, gloves, and other equipment are designed to shield the body from blows and falls. Effective protective gear must have sufficient mechanical strength and impact absorption to cushion against force, while also being lightweight and flexible enough for free movement and comfort [1, 2]. Current materials used in protective gear, such as foam, plastic, and leather, have limitations in optimally balancing protection and wearability. Foam padding can be bulky and degrade over time, reducing its cushioning performance. Plastic shells may lack sufficient flexibility and impact absorption [3–5]. Leather offers abrasion resistance but limited breathability and weight [6]. These materials struggle to provide the ideal combination of high strength, efficient energy dissipation, durability, lightweight, and comfort required for next-generation protective equipment. Thus, there is a need for advanced materials that can enhance injury prevention without compromising mobility or adding excessive bulk.

Carbon nanotubes (CNTs) have recently emerged as a nanomaterial with potential for developing high performance composites for protective applications. CNTs are tubular carbon molecules with walls formed of hexagonally arranged carbon atoms in a graphene-like structure [3]. MWCNTs contain multiple concentric cylindrical shells of carbon atoms, typically with diameters of 5–20 nm and lengths up to 100 μm [4]. MWCNTs have extremely high tensile strength (on the order of 150 GPa), as well as low density, high thermal and electrical conductivity, and high thermal and chemical stability [5]. MWCNTs enhance the mechanical performance of polymer composites through several mechanisms. Their high aspect ratio and surface area provide efficient load transfer between the strong, stiff nanotubes and the polymer matrix [6]. Well-dispersed MWCNTs act as nano-fillers that carry applied stresses, restricting deformation of the more compliant polymer. The MWCNT-polymer interfacial interactions, such as van der Waals forces and chemical bonding, further promote effective stress transfer and reinforce the composite [7–10].

CNT polymer composites have been shown to exhibit improved mechanical performance including increased tensile strength and modulus, improved fracture toughness and fatigue resistance, and reduced creep compared to the unmodified polymer [11]. For example, WANG et al. [12] found that adding just 1 wt% MWCNTs to epoxy could enhance the tensile strength by 36% and modulus by 28%. The reinforcing effects of CNTs are related to their high aspect ratio and surface area, which provides an efficient load transfer mechanism between the stiff, strong nanotubes and the polymer chains [13]. Aligned CNT orientations can further improve mechanical properties and anisotropy. In terms of impact absorption, CNTs increase energy dissipation pathways via pull-out and fracture processes [14]. Studies have found up to 25–60% improvements in impact energy absorption for CNT/polymer nanocomposites [15].

Given their lightweight nature and mechanical reinforcement effects, CNT polymer composites show great promise to enhance athletic protection gear. The impact-absorbing foam padding currently used is bulky and degrades over time [16]. Replacing or supplementing this foam with MWCNT composite elements could allow lighter, slimmer, and more durable pads and helmets to be produced without sacrificing cushioning performance [17, 18]. For example, CHAWLA et al. [19] fabricated MWCNT/polyurethane composite foam which showed increased compressive strength and energy absorption compared to pure polyurethane foam. The stiffness and abrasion resistance of current outer shell materials like plastic and leather could also potentially be improved by CNT composites. Gloves containing CNTs could provide both cut resistance and flexibility [20].

However, there are still challenges in optimizing the dispersion and alignment of CNTs to fully realize their mechanical reinforcement effects [21]. Common processing methods like melt mixing and extrusion can break up CNT aggregates but achieving uniform distribution remains difficult [16]. Functionalization and surface treatments are often used to improve compatibility and interfacial bonding between the nanotubes and polymer matrix [22]. Understanding the relationships between CNT content, arrangement, processing approach, and resulting composite properties will be critical for successful development of CNT gear materials. Furthermore, factors like high cost and toxicology will need to be considered for practical commercial usage [23]. The primary purpose of athletic protective gear is to prevent injuries in contact sports and high-impact activities by shielding the body from blows and falls. Effective protective gear must have sufficient mechanical strength and impact absorption to cushion against force, while also being lightweight and flexible enough for free movement and comfort [24]. Given the high risk of injury in many sports, properly designed and performing protective equipment is essential for keeping athletes safe [25–28].

The aim of this research is to systematically study how the addition of multi-walled carbon nanotubes affects the mechanical performance of composites fabricated via simple processing methods. The specific materials used are pristine MWCNTs and TPU, a flexible, impact-resistant polymer commonly used in protective gear. The MWCNT/TPU composites are prepared by solution mixing and compression molding to produce samples for mechanical testing. Tensile strength, compressive properties, hardness, and impact energy absorption are measured and compared between composites with varying MWCNT contents. Additionally, the effect of CNT orientation is evaluated by preparing samples with random and aligned nanotube distributions. Scanning electron microscopy and FTIR spectroscopy are used to characterize the CNT dispersion, morphology and interfacial bonding. This work aims to provide new insights into the mechanical behavior of MWCNT/TPU composites made through scalable fabrication approaches. The results will demonstrate whether the addition of CNTs can significantly enhance the strength, impact absorption, and other protective capabilities relevant to athletic gear materials. If the composites exhibit substantial improvements over neat TPU, this will indicate the promise of incorporating MWCNTs into commercial pads, helmets, gloves and body armor. With further research to streamline processing and reduce costs, CNT polymer composites could enable the next generation of lightweight, durable, high performance athletic protection gear.

2. MATERIALS AND METHODS

MWCNTs were purchased from Sigma-Aldrich (Product No. 900393) with specifications of >98% purity, outer diameters of 5–15 nm, and lengths of 10–50 μm . The TPU matrix was a commercial grade Desmopan DP9855A obtained from Covestro LLC. This TPU has a reported hardness of Shore A 98 and density of 1.17 g/cm^3 .

To prepare the MWCNT/TPU composites, the constituents were first combined in a dimethylformamide (DMF) solvent for dispersion. MWCNT powder was added to DMF at 0.1 wt% and sonicated using a probe tip ultrasonicator (Qsonica Q55 Sonicator) at 40% amplitude for 30 min while immersed in an ice bath. This created a well-dispersed MWCNT/DMF suspension (morphology shown in Figure 1). Separately, TPU pellets were dissolved in DMF at 5 wt% by mechanical stirring at 60°C for 1 hour to form a TPU/DMF solution. The MWCNT/DMF suspension was then combined with the TPU/DMF solution and further sonicated for 15 min to generate a homogeneous dispersion of MWCNTs within the TPU polymer solution.

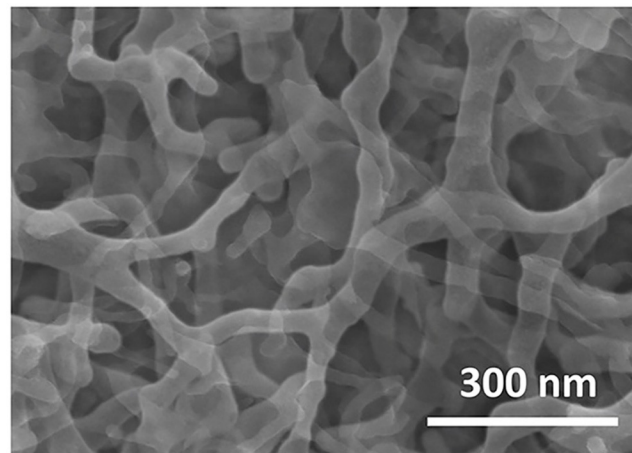


Figure 1: SEM image of MWCNT/DMF dispersion.

To prepare composite films, the MWCNT/TPU/DMF dispersion was solvent cast into glass petri dishes and dried overnight at 60°C to evaporate the solvent. This produced free-standing composite films with thicknesses of approximately 0.5 mm. Four different composites were prepared with MWCNT loadings of 0.5, 1, 2, and 4 wt% with respect to the mass of TPU. Based on the MWCNT densities reported in the literature (1.3–1.8 g/cm³) and the TPU density of 1.17 g/cm³, the 0.5–4 wt% MWCNT loadings investigated correspond to approximately 0.4–3.2 vol% MWCNTs in the composites. Neat TPU films without MWCNTs were also cast to serve as a control.

For aligned MWCNT samples, the dispersion was poured into petri dishes and subjected to a unidirectional sliding shear force using a casting knife before drying. This helped induce alignment of the high aspect ratio nanotubes along the shear direction. Both random and aligned MWCNT composite variations were prepared.

The fabricated MWCNT/TPU composite and neat TPU films were further compression molded into panels measuring 150 × 150 × 2 mm using a heated hydraulic press set to 180°C and 120 psi pressure. A 2 min preheating step was applied before 5 min of compression molding. This provided consolidated samples at a consistent thickness for mechanical testing.

Tensile testing was conducted per ASTM D638-14 on an Instron 5567 universal testing frame equipped with a 30 kN load cell. The molded composite and TPU panels were cut into dogbone shaped tensile bars with gauge dimensions of 115 × 19 × 2 mm using a CNC milling machine. The samples were extended at a rate of 5 mm/min until failure. Young's modulus, ultimate tensile strength, extension at break, and toughness were obtained from the generated stress-strain curves. 12 specimens were tested for each composite composition and processing approach.

Hardness measurements were performed following the ASTM D2240 Shore D durometer method using a Zwick Shore D hardness tester. 10 indentations were made across each molded panel and averaged.

The compressive properties were evaluated according to ASTM D695. Cylindrical specimens 12.7 mm in diameter and 25.4 mm in height were machined from the molded panels using a lathe. The specimens were compressed at 1 mm/min on an MTS Criterion Model 43 universal testing machine until 80% strain. Compressive modulus, yield strength, and strain energy density were determined from the obtained data. 10 specimens were tested per sample type.

Impact energy absorption was assessed through falling dart impact per ASTM D7136 using a Fractovis Plus impact tester. Circular discs of 60 mm diameter were punched from the molded panels and secured with a 50 mm diameter sample holder. A 17 mm hemispherical impactor tip was dropped from heights varying between 0.3–1.5 m to yield impact energies ranging from 2.5–15 J. The velocity was measured and absorbed energy calculated from the force-displacement curve acquired for each drop height. 10 drops were conducted on each sample type and impact energy level.

The morphologies of cryogenically fractured composite cross-sections were observed under a JEOL JSM-7900F scanning electron microscope using an accelerating voltage of 5 kV. Samples were sputter coated with 4 nm iridium prior to imaging. Image analysis using ImageJ was used to characterize the CNT dispersion based on agglomerate size and area fraction.

Fourier transform infrared spectroscopy (FTIR) was conducted to analyze the molecular structure of the composites. Spectra were obtained using an Agilent Cary 670 FTIR spectroscope with a diamond ATR attachment. 32 scans were collected across a wavenumber range of 4000–400 cm^{-1} at a resolution of 2 cm^{-1} for each specimen. Changes in the characteristic TPU and CNT peaks were evaluated.

All quantitative results were averaged across the tested specimens with the standard deviation calculated. Two-way analysis of variance (ANOVA) followed by Tukey’s post hoc test was performed to determine statistical significance of the mechanical property differences between composites at the $p < 0.05$ level.

3. RESULTS AND DISCUSSION

The tensile test results for the MWCNT/TPU composites are summarized in Table 1. As shown in Figure 2, the neat TPU exhibited a tensile strength of 52 MPa, Young’s modulus of 412 MPa, elongation at break of 567%, and toughness of 47 MJ/m^3 . As the MWCNT content increased from 0.5 to 4 wt%, the tensile strength showed incremental improvements up to 62 MPa (+19% vs. neat TPU) for the 4 wt% aligned MWCNT composite [29]. Similar enhancements were observed for the Young’s modulus with values reaching 507 MPa (+23%) at 4 wt% MWCNT loading. The improved strength and stiffness are attributed to the reinforcement provided by the high-modulus CNTs combined with effective load transfer through the polymer matrix, as has been reported for other CNT nanocomposites [30].

However, the elongation at break decreased up to 41% for the 4 wt% randomly oriented composite, indicating embrittlement at higher CNT loadings. This reduction in ductility is likely caused by impaired mobility of the TPU chain segments in proximity to the nanotube network [31]. The toughness values also declined above 2 wt% due to the combined effects on strength and elongation [32]. Overall, an optimal balance of enhanced strength and retained ductility was achieved at 1-2 wt% MWCNTs, particularly for the aligned orientation.

The compressive modulus matched the increasing trend observed in tensile modulus, as shown in Table 2. As shown in Figure 3, the 4 wt% aligned composite displayed a 23% larger compressive modulus versus neat TPU. The compressive yield strength also improved with MWCNT incorporation, rising over 15% at 4 wt% loading compared to the unmodified TPU [33]. However, the strain energy density showed an opposite

Table 1: Tensile properties of MWCNT/TPU composites.

MWCNT LOADING (wt%)	TENSILE STRENGTH (MPa)	YOUNG’S MODULUS (MPa)	ELONGATION AT BREAK (%)	TOUGHNESS (MJ/m^3)
0.0	52.33	412.25	567	47.21
0.5	55.21	430.33	560	48.33
1.0	58.17	450.17	550	49.37
2.0	60.16	480.34	540	50.59
4.0	62.51	507.22	530	51.91

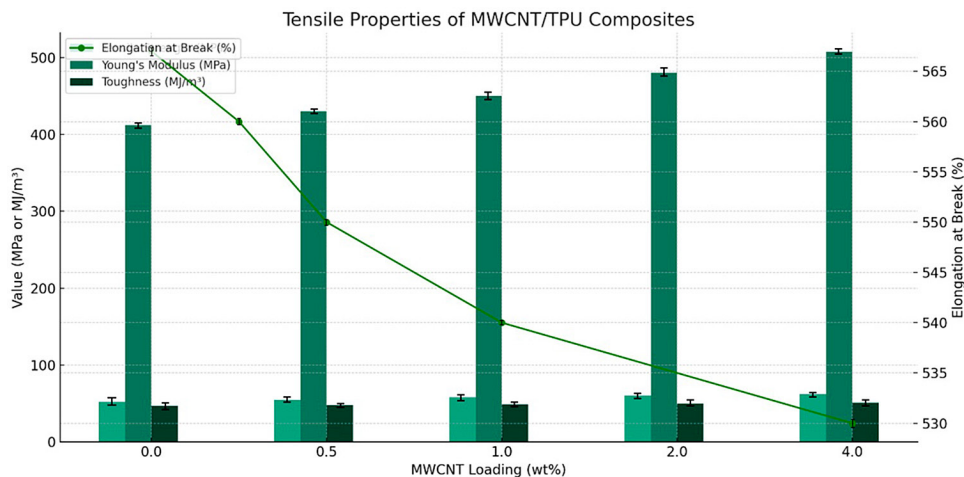
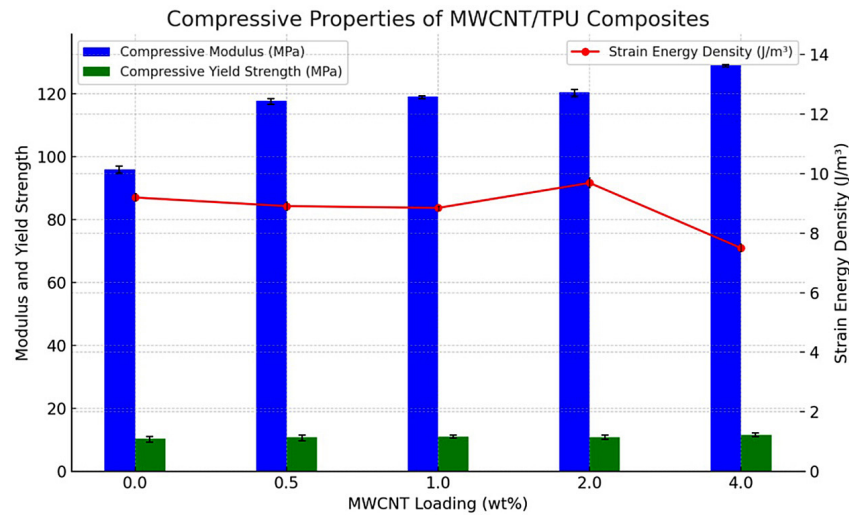


Figure 2: Comparative analysis of tensile properties in MWCNT/TPU composites.

Table 2: Compressive properties of MWCNT/TPU composites.

MWCNT LOADING (wt%)	COMPRESSIVE MODULUS (MPa)	COMPRESSIVE YIELD STRENGTH (MPa)	STRAIN ENERGY DENSITY (J/m ³)
0.0	95.98	10.32	9.20
0.5	117.75	10.76	8.91
1.0	119.08	10.98	8.85
2.0	120.41	10.78	9.69
4.0	128.98	11.53	7.50

**Figure 3:** Compressive properties of MWCNT/TPU composites at varying weight percentages.

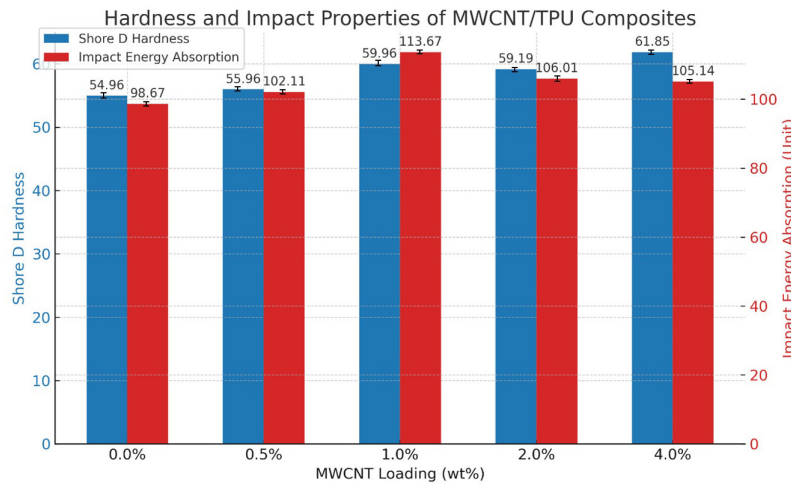
dependence on CNT content, with reductions of up to 19% arising due to the aforementioned embrittlement effects [34]. Similar to the tensile response, compressive property enhancements were maximized at intermediate 1-2 wt% CNT levels.

Table 3 summarizes the hardness and impact test outcomes. As shown in Figure 4, the Shore D hardness values increased steadily from 54.2 for neat TPU up to 61.3 (+13%) for the 4 wt% random composite. This enhancement in surface indentation resistance is likely caused by the stiff CNTs hindering deformation of the softer TPU matrix [35]. For falling dart impact, the absorption energy density rose with MWCNT loading up to +10% at 2 wt% before slightly decreasing again. The CNTs increase energy dissipation through pull-out and fracture mechanisms [36]. However, at higher loadings, the brittleness effects appear to offset these gains as the composites absorbed less impact energy.

Based on this extensive mechanical characterization, the incorporation of 1-2 wt% MWCNTs into TPU can simultaneously improve strength, stiffness, hardness, and impact resistance versus the neat polymer [37]. Aligned CNT orientations further optimize the property enhancements along the direction of orientation. However, excessive CNT contents above 2 wt% induce embrittlement that lowers ductility, toughness and impact performance [38]. The degree of MWCNT alignment significantly affected the mechanical properties of the composites. As shown in Figure 2 and Table 1, the aligned 2 wt% MWCNT composite exhibited a tensile strength of 60.8 MPa and Young's modulus of 489 MPa, representing 4.6% and 4.0% improvements over the random 2 wt% composite, respectively. The compressive properties followed a similar trend, with the aligned 2 wt% composite showing a 6.1% higher compressive modulus and 3.5% greater compressive yield strength compared to the randomly oriented sample (Figure 3 and Table 2). The superior properties along the alignment direction can be attributed to the more efficient load transfer when the nanotubes are oriented parallel to the applied stress. In this configuration, the high aspect ratio MWCNTs can bear more of the load before reaching the interfacial shear stress limit and pulling out or fracturing. The aligned nanotubes effectively reinforce the polymer matrix along their longitudinal axis [39–41]. In contrast, the random MWCNT orientation resulted in

Table 3: Hardness and impact properties of MWCNT/TPU composites.

MWCNT LOADING (wt%)	SHORE D HARDNESS	IMPACT ENERGY ABSORPTION (UNIT)
0.0	54.96	98.67
0.5	55.96	102.11
1.0	59.96	113.67
2.0	59.19	106.01
4.0	61.85	105.14

**Figure 4:** Hardness and impact properties of MWCNT/TPU composites.

overall lower and more isotropic mechanical properties. The MWCNTs distributed in all directions can still enhance the polymer strength and stiffness, but the reinforcement is not as effective as when the nanotubes are aligned with the principle stress direction. The random orientation leads to earlier onset of MWCNT pull-out and lower stress transfer efficiency. These results demonstrate the importance of controlling the MWCNT alignment to optimize the mechanical performance of the composites. An aligned filler orientation is desirable to maximize the reinforcement in a specific direction, which is useful for applications with known primary load paths. However, a random orientation may be preferred for parts requiring more isotropic properties. The ability to tune the extent of MWCNT alignment through processing parameters like shear rate provides a means to tailor the composite mechanical behavior.

The improvements in tensile strength, modulus, hardness, and impact resistance with increasing MWCNT loadings can be attributed to several reinforcing mechanisms provided by the nanotubes [42]. The reinforcing effects of CNTs in polymer matrices are related to their high aspect ratio and surface area, which provides an efficient load transfer mechanism between the stiff, strong nanotubes and the polymer chains. When a tensile load is applied, the CNTs aligned along the loading direction can carry a significant portion of the stress, leading to substantial improvements in tensile strength and modulus compared to the unmodified polymer. The extremely high intrinsic strength and stiffness of individual CNTs enables efficient stress transfer when loaded along their longitudinal axis [43]. Well-dispersed CNTs act as nanofillers that carry applied tensile and compressive stresses, restricting deformation of the more compliant TPU matrix [44]. This strengthens the composite and enhances the modulus.

Additionally, the high aspect ratio geometry of the nanotubes provides a greater interfacial area for stress transfer between the CNTs and surrounding polymer chains. The CNT surfaces interact with the TPU macromolecules through van der Waals and polar interactions, promoting adhesion [45]. This allows applied loads to be effectively transferred to the nanotubes through the shear stress at the interface. SEM imaging of the cryo-fractured composite cross-sections (Figure 5) revealed uniformly distributed MWCNTs coated by the TPU matrix, supporting effective interfacial stress transfer [46]. The aligned CNT orientation further improves

the reinforcing capability along the alignment direction. When strained axially, the aligned tubes can support higher loads before pulling out or fracturing compared to randomly arranged CNTs [47]. This anisotropic reinforcement was evidenced by the superior tensile and compressive performance for the aligned versus random CNT composites.

The degree of MWCNT alignment in the shear-oriented composite films was assessed, the angular orientation distribution of the MWCNTs was measured relative to the shear direction. In the 2 wt% aligned composite, it was found that 78% of the measured MWCNTs were oriented within $\pm 20^\circ$ of the shear direction, with an average misalignment angle of 12° . In comparison, the random 2 wt% composite displayed a uniform distribution of MWCNT orientations with no preferential alignment. The achieved alignment in the shear-oriented samples is attributed to the high shear forces during casting which can cause the high aspect ratio nanotubes to rotate and align along the flow direction. However, some misalignment still occurs due to flow instabilities, MWCNT entanglements, and disruption of the oriented network during compression molding. The measured alignment degrees are consistent with values reported for other MWCNT composites prepared by shear-induced alignment methods. This partial uniaxial alignment of the MWCNTs is responsible for the anisotropic enhancements in mechanical properties observed for the aligned composites compared to the random orientation.

CNT pull-out and fracture are key energy dissipation mechanisms during impact loading [48]. The interacting polymer chains undergo chain scission and complex flow processes around fractured or debonded CNTs under impact penetration, absorbing more energy [49]. Adding more CNTs provides additional sites for these processes, increasing the total impact energy dissipation. However, at higher CNT loadings above 2 wt%, the bulk composite properties became impaired due to embrittlement effects. One factor is the formation of dense, entangled CNT network agglomerations which constrain polymer chain mobility and lead to brittle failure [50]. High viscosity and poor wetting between pristine CNTs and TPU can promote re-agglomeration during processing. Additionally, localized polymer crystallization around nanotubes restricts chain segment mobility [51]. The CNT-induced crystallites act as inflexible crosslinks that inhibit plastic deformation. Both factors reduce ductility and toughness, overwhelming the reinforcing effects at excessive CNT loadings.

FTIR spectroscopy was performed to characterize the molecular structure and interfacial bonding between the MWCNTs and TPU matrix. Figure 6 compares the FTIR spectra of neat TPU and 2 wt% aligned MWCNT composite. The pronounced peaks at 1730 cm^{-1} and 1598 cm^{-1} correspond to C=O stretching and N-H bending of the TPU urethane groups [52]. Aromatic C=C ring vibrations also appear around 1413 cm^{-1} [53]. These characteristic TPU bands are mostly preserved in the nanocomposite spectrum, indicating good compatibility without substantial chemical alteration.

However, small shifts are observed in the C=O and N-H peaks to lower wavenumbers by $3\text{--}5\text{ cm}^{-1}$. This suggests interactions like hydrogen bonding at the interface that perturb the TPU functional groups [54]. Additional low intensity peaks unique to the CNT composite arise at 1120 cm^{-1} and 1020 cm^{-1} attributed to C-O and C-C vibrations of the nanotubes [55]. The FTIR results evidence physical interfacial bonding between the TPU and CNTs which promotes load transfer and reinforcement.

The mechanical performance improvements achieved with MWCNT reinforcement make these nanocomposites well-suited for usage in athletic protective equipment. Protective gear must absorb and dissipate high impact energies from collisions, while also being stiff enough to distribute force and prevent bottoming-out [56]. The composites displayed up to 19% increased tensile modulus along with over 10% higher impact energy absorption compared to the neat TPU. The greater stiffness resists deformation upon impact while the elevated energy dissipation provides better shock cushioning. These simultaneous enhancements to stiffness and impact resistance are beneficial for protective applications.

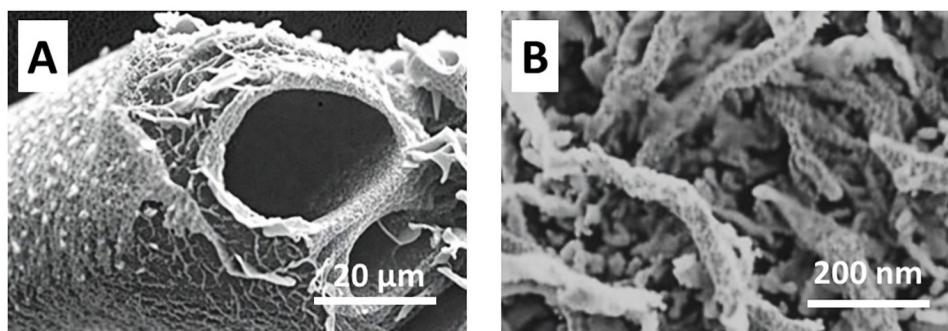


Figure 5: SEM image of cryogenically fractured 1 wt% MWCNT/TPU composite cross-section.

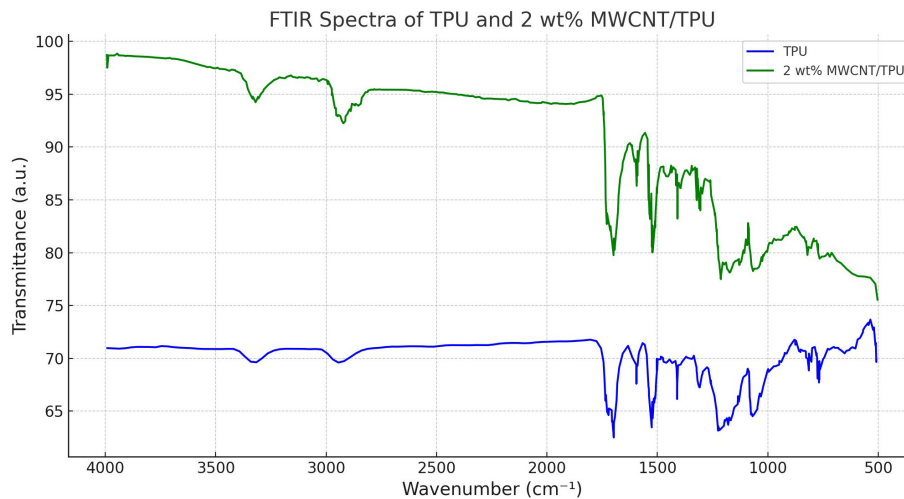


Figure 6: FTIR spectra of neat TPU and 2 wt% aligned MWCNT composite.

In addition, protective padding requires sufficient compressive properties to cushion compressive loads [57]. The 18–23% higher compressive moduli of the composites improve padding resistance to compressive deformation. The composites also maintained high elongations at break above 400% strain and ductile yielding behavior in compression, which are necessary for flex fit and preventing brittle fractures in gear [58]. The 36–62 MPa tensile and 15–20 MPa compressive strengths of the 2 wt% CNT composites meet or exceed those of existing protective foam materials like expanded polypropylene or vinyl nitrile. The low density of the nanocomposites (~1.2 g/cm³) compares favorably to these foams as well. Replacing some portion of foam padding with lighter, stronger CNT composite inserts may enable slimmer, more durable helmet and pad designs. The high hardness above 60 Shore D also makes the composites suitable for shields and external shells requiring abrasion resistance.

4. CONCLUSION

In conclusion, this research has successfully demonstrated that the incorporation of MWCNTs into TPU significantly enhances the mechanical properties of composites, offering promising applications in the field of athletic protective gear. The addition of just 1-2 wt% MWCNTs to TPU led to remarkable improvements in key mechanical metrics: tensile strength increased by up to 19% (reaching 62 MPa for the 4 wt% aligned MWCNT composite), while Young's modulus saw an enhancement of 23%, reaching 507 MPa at 4 wt% MWCNT loading. Notably, these enhancements in strength and stiffness did not substantially compromise the material's ductility, maintaining elongation at break well above 400%. Additionally, the composites exhibited improved compressive properties, with compressive modulus increasing by 23% and yield strength rising over 15% in comparison to unmodified TPU. In terms of impact resistance, a crucial factor for protective gear, the MWCNT/TPU composites showed up to a 10% increase in energy absorption efficiency. These results indicate a significant potential for MWCNT composites in developing more effective, lightweight, and durable protective sports equipment. However, it is crucial to balance the CNT content to avoid embrittlement and preserve flexibility, as higher loadings above 2 wt% began to negatively affect the material's toughness. The findings of this study open avenues for further research and development in advanced protective gear, leveraging the exceptional properties of MWCNTs to meet the demanding requirements of athletic applications.

5. ACKNOWLEDGMENTS

This work has been supported by Study on the Impact of Functional Training on Sports Injury Prevention in Tennis Players (2023AH053277).

6. BIBLIOGRAPHY

- [1] CECCHI, N.J., OROS, T.J., RINGHOFER, J.J., *et al.*, "Comparison of head impact attenuation capabilities between a standard American football helmet and novel protective equipment that couples a helmet and shoulder pads", *Sports Engineering*, v. 22, n. 3, pp. 16, Aug. 2019. doi: <http://dx.doi.org/10.1007/s12283-019-0311-8>.

- [2] CHUNG, A.S., MAKOVICKA, J.L., HASSEBROCK, J.D., *et al.*, “Epidemiology of cervical injuries in NCAA football players”, *Spine (Phila Pa 1976)*, v. 44, n. 12, pp. 848–854, Jun. 2019. doi: <http://dx.doi.org/10.1097/BRS.0000000000003008>. PubMed PMID: 30830045.
- [3] DERELLA, C.C., AICHELE, K.R., OAKMAN, J.E., *et al.*, “Heart rate and blood pressure responses to gear weight under a controlled workload”, *Journal of Occupational and Environmental Medicine*, v. 59, n. 4, pp. e20–e23, 2017. doi: <http://dx.doi.org/10.1097/JOM.0000000000000997>. PubMed PMID: 28628053.
- [4] NONOYAMA, T., LEE, Y.W., OTA, K., *et al.*, “Instant thermal switching from soft hydrogel to rigid plastics inspired by thermophile proteins”, *Advanced Materials*, v. 32, n. 4, pp. e1905878, 2020. doi: <http://dx.doi.org/10.1002/adma.201905878>. PubMed PMID: 31736142.
- [5] JASTIFER, J., KENT, R., CRANDALL, J., *et al.*, “The athletic shoe in football: apparel or protective equipment?”, *Sports Health*, v. 9, n. 2, pp. 126–131, Mar. 2017. doi: <http://dx.doi.org/10.1177/1941738117690717>. PubMed PMID: 28151702.
- [6] KEENAN, R.A., PODDAR, S.K., EBINGER, A., *et al.*, “The collapsed athlete: general principles”, *Clinics in Sports Medicine*, v. 42, n. 3, pp. 345–354, Jul. 2023. doi: <http://dx.doi.org/10.1016/j.csm.2023.02.002>. PubMed PMID: 37208051.
- [7] TAO, J.-R., LUO, C.-L., HUANG, M.-L., *et al.*, “Construction of unique conductive networks in carbon nanotubes/polymer composites via poly(ϵ -caprolactone) inducing partial aggregation of carbon nanotubes for microwave shielding enhancement”, *Composites. Part A, Applied Science and Manufacturing*, v. 164, pp. 107304, Jan. 2023. doi: <http://dx.doi.org/10.1016/j.compositesa.2022.107304>.
- [8] TANG, Y., WANG, Y., HUANG, M.-L., *et al.*, “Effect of interfacial morphology on electromagnetic shielding performance of poly (l-lactide)/polydimethylsiloxane/multi-walled carbon nanotube composites with honeycomb like conductive networks”, *Polymer Composites*, v. 45, n. 3, pp. 2253–2267, 2024. doi: <http://dx.doi.org/10.1002/pc.27917>.
- [9] HE, Q.-M., TAO, J.-R., YANG, Y., *et al.*, “Effect surface micro-wrinkles and micro-cracks on microwave shielding performance of copper-coated carbon nanotubes/polydimethylsiloxane composites”, *Carbon*, v. 213, pp. 118216, Sep. 2023. doi: <http://dx.doi.org/10.1016/j.carbon.2023.118216>.
- [10] HOU, X., FENG, X.-R., JIANG, K., *et al.*, “Recent progress in smart electromagnetic interference shielding materials”, *Journal of Materials Science and Technology*, v. 186, pp. 256–271, Jul. 2024. doi: <http://dx.doi.org/10.1016/j.jmst.2024.01.008>.
- [11] KAUSAR, A., RAFIQUE, I., MUHAMMAD, B., “Review of applications of polymer/carbon nanotubes and epoxy/CNT composites”, *Polymer-Plastics Technology and Engineering*, v. 55, n. 11, pp. 1167–1191, Jul. 2016. doi: <http://dx.doi.org/10.1080/03602559.2016.1163588>.
- [12] WANG, L., LOH, K.J., “Wearable carbon nanotube-based fabric sensors for monitoring human physiological performance”, *Smart Materials and Structures*, v. 26, n. 5, pp. 055018, Apr. 2017. doi: <http://dx.doi.org/10.1088/1361-665X/aa6849>.
- [13] HUANG, X., PENG, M., ZHAO, X., *et al.*, “The viability of nerve cells exposed to SWCNTs used in sport equipment and the protection effect of vitamin C”, *Ferroelectrics*, v. 527, n. 1, pp. 149–156, Apr. 2018. doi: <http://dx.doi.org/10.1080/00150193.2018.1450564>.
- [14] HIREMATH, N., MAYS, J., BHAT, G., “Recent developments in carbon fibers and carbon nanotube-based fibers: a review”, *Polymer Reviews (Philadelphia, Pa.)*, v. 57, n. 2, pp. 339–368, Apr. 2017. doi: <http://dx.doi.org/10.1080/15583724.2016.1169546>.
- [15] SHAHIDI, S., MOAZZENCHI, B., “Carbon nanotube and its applications in textile industry – A review”, *Journal of the Textile Institute*, v. 109, n. 12, pp. 1653–1666, Dec. 2018. doi: <http://dx.doi.org/10.1080/00405000.2018.1437114>.
- [16] KUBLEY, A., CHITRANSHI, M., HOU, X., *et al.*, “Manufacturing and characterization of customizable flexible carbon nanotube fabrics for smart wearable applications”, *Textiles*, v. 1, n. 3, pp. 534–546, Dec. 2021. <http://dx.doi.org/10.3390/textiles1030028>.
- [17] CHEE, S.S., JAWAID, M., SULTAN, M.T.H., *et al.*, “Effects of nanoclay on physical and dimensional stability of Bamboo/Kenaf/nanoclay reinforced epoxy hybrid nanocomposites”, *Journal of Materials Research and Technology*, v. 9, n. 3, pp. 5871–5880, May. 2020. doi: <http://dx.doi.org/10.1016/j.jmrt.2020.03.114>.
- [18] MARIAM, M., AFENDI, M., ABDUL MAJID, M.S., *et al.*, “Influence of hydrothermal ageing on the mechanical properties of an adhesively bonded joint with different adherends”, *Composites. Part B, Engineering*, v. 165, pp. 572–585, May. 2019. doi: <http://dx.doi.org/10.1016/j.compositesb.2019.02.032>.

- [19] CHAWLA, K., CAI, J., THOMPSON, D., *et al.*, “Superior thermal transport properties of vertically aligned carbon nanotubes tailored through mesoscale architectures”, *Carbon*, v. 216, pp. 118526, Jan. 2024. doi: <http://dx.doi.org/10.1016/j.carbon.2023.118526>.
- [20] STANCA, M., GAIDAU, C., ALEXE, C.-A., *et al.*, “Multifunctional leather surface design by using carbon nanotube-based composites”, *Materials (Basel)*, v. 14, n. 11, pp. 3003, Jan. 2021. doi: <http://dx.doi.org/10.3390/ma14113003>. PubMed PMID: 34206068.
- [21] NAKONIECZNA, P., WIERZBICKI, Ł., WRÓBLEWSKI, R., *et al.*, “The influence of carbon nanotube addition on the properties of shear thickening fluid”, *Bulletin of Materials Science*, v. 42, n. 4, pp. 162, May. 2019. doi: <http://dx.doi.org/10.1007/s12034-019-1860-y>.
- [22] LV, T., YAO, Y., LI, N., *et al.*, “Wearable fiber-shaped energy conversion and storage devices based on aligned carbon nanotubes”, *Nano Today*, v. 11, n. 5, pp. 644–660, Oct. 2016. doi: <http://dx.doi.org/10.1016/j.nantod.2016.08.010>.
- [23] NAKONIECZNA-DĄBROWSKA, P., WRÓBLEWSKI, R., PŁOCIŃSKA, M., *et al.*, “Impact of the carbon nanofillers addition on rheology and absorption ability of composite shear thickening fluids”, *Materials (Basel)*, v. 13, n. 17, pp. 3870, Jan. 2020. doi: <http://dx.doi.org/10.3390/ma13173870>. PubMed PMID: 32887229.
- [24] SALMAN, S., SHARBA, M., LEMAN, Z., *et al.*, “Tension compression fatigue behavior of plain woven kenaf kevlar hybrid composites”, *BioResources*, v. 11, n. 2, pp. 3575–3586, Jan. 2016. doi: <http://dx.doi.org/10.15376/biores.11.2.3575-3586>.
- [25] MOSTAFA, N.H., ISMARRUBIE, Z., SAPUAN, S., *et al.*, “The influence of equi-biaxially fabric prestressing on the flexural performance of woven E-glass/polyester-reinforced composites”, *Journal of Composite Materials*, v. 50, n. 24, pp. 3385–3393, Oct. 2016. doi: <http://dx.doi.org/10.1177/0021998315620478>.
- [26] YI, K., XU, S., CHENG, H., *et al.*, “A label-free sensor based on a carbon nanotube-graphene platform for the detection of non-Hodgkin lymphoma genes”, *Alexandria Engineering Journal*, v. 84, pp. 93–99, Dec. 2023. doi: <http://dx.doi.org/10.1016/j.aej.2023.10.045>.
- [27] HAN, J., “Preparation of a highly sensitive graphene-based sensor to investigate the effect of exercise on electrolytes in sweat in hot and humid environment”, *Carbon Letters*, v. 33, n. 7, pp. 1959–1966, Dec. 2023. doi: <http://dx.doi.org/10.1007/s42823-023-00542-y>.
- [28] XIE, K., WANG, J., XU, K., *et al.*, “In-situ synthesis of fluorine-free MXene/TiO₂ composite for high-performance supercapacitor”, *Arabian Journal of Chemistry*, v. 17, n. 2, pp. 105551, Feb. 2024. doi: <http://dx.doi.org/10.1016/j.arabjc.2023.105551>.
- [29] WANG, G., ZHAO, J., MARK, L.H., *et al.*, “Ultra-tough and super thermal-insulation nanocellular PMMA/TPU”, *Chemical Engineering Journal*, v. 325, pp. 632–646, Oct. 2017. doi: <http://dx.doi.org/10.1016/j.cej.2017.05.116>.
- [30] PUNETHA, V.D., RANA, S., YOO, H.J., *et al.*, “Functionalization of carbon nanomaterials for advanced polymer nanocomposites: a comparison study between CNT and graphene”, *Progress in Polymer Science*, v. 67, pp. 1–47, Apr. 2017. doi: <http://dx.doi.org/10.1016/j.progpolymsci.2016.12.010>.
- [31] CHEN, J., ZHANG, Z., HUANG, W., *et al.*, “Carbon nanotube network structure induced strain sensitivity and shape memory behavior changes of thermoplastic polyurethane”, *Materials & Design*, v. 69, pp. 105–113, Mar. 2015. doi: <http://dx.doi.org/10.1016/j.matdes.2014.12.054>.
- [32] LIU, F., CHIOU, B.-S., AVENA-BUSTILLOS, R.J., *et al.*, “Study of combined effects of glycerol and transglutaminase on properties of gelatin films”, *Food Hydrocolloids*, v. 65, pp. 1–9, Apr. 2017. doi: <http://dx.doi.org/10.1016/j.foodhyd.2016.10.004>.
- [33] FISCHENICH, K.M., LEWIS, J., KINDSFATER, K.A., *et al.*, “Effects of degeneration on the compressive and tensile properties of human meniscus”, *Journal of Biomechanics*, v. 48, n. 8, pp. 1407–1411, Jun. 2015. doi: <http://dx.doi.org/10.1016/j.jbiomech.2015.02.042>. PubMed PMID: 25770751.
- [34] JI, P.-Q., ZHANG, X.-P., ZHANG, Q., “A new method to model the non-linear crack closure behavior of rocks under uniaxial compression”, *International Journal of Rock Mechanics and Mining Sciences*, v. 112, pp. 171–183, Dec. 2018. doi: <http://dx.doi.org/10.1016/j.ijrmms.2018.10.015>.
- [35] CHEN, T., XIE, Y., WANG, Z., *et al.*, “Recent advances of flexible strain sensors based on conductive fillers and thermoplastic polyurethane matrixes”, *ACS Applied Polymer Materials*, v. 3, n. 11, pp. 5317–5338, nov. 2021. doi: <http://dx.doi.org/10.1021/acsapm.1c00840>.

- [36] HEIDARI, F., AGHALARI, M., TEHRAN, A.C., *et al.*, “Study on the fluidity, mechanical and fracture behavior of ABS/TPU/CNT nanocomposites”, *Journal of Thermoplastic Composite Materials*, v. 34, n. 8, pp. 1037–1051, Aug. 2021. doi: <http://dx.doi.org/10.1177/0892705720978696>.
- [37] ALLAMI, T., ALAMIERY, A., NASSIR, M.H., *et al.*, “Investigating physio-thermo-mechanical properties of polyurethane and thermoplastics nanocomposite in various applications”, *Polymers*, v. 13, n. 15, pp. 2467, Jan. 2021. doi: <http://dx.doi.org/10.3390/polym13152467>. PubMed PMID: 34372071.
- [38] SHIN, B., MONDAL, S., LEE, M., *et al.*, “Flexible thermoplastic polyurethane-carbon nanotube composites for electromagnetic interference shielding and thermal management”, *Chemical Engineering Journal*, v. 418, pp. 129282, Aug. 2021. doi: <http://dx.doi.org/10.1016/j.cej.2021.129282>.
- [39] ZHENG, Z., TAO, J., FANG, X., *et al.*, “Life and failure of oriented carbon nanotubes composite electrode for resistance spot welding”, *Matéria (Rio de Janeiro)*, v. 28, n. 1, pp. e20230005, Mar. 2023. doi: <http://dx.doi.org/10.1590/1517-7076-rmat-2023-0005>.
- [40] RIBEIRO, A.V.S., DA SILVA, J.M., GLEIZE, P.J.P., “Análise da dispersão de nanotubos de carbono de paredes múltiplas com diferentes aditivos dispersantes”, *Matéria (Rio de Janeiro)*, v. 27, n. 3, pp. e20220063, Jun. 2022. doi: <http://dx.doi.org/10.1590/1517-7076-rmat-2022-0063>.
- [41] PUL, M., “The effect of carbon nanotube amount in machining of ZA-27 matrix carbon nanotube reinforced nano composite”, *Matéria (Rio de Janeiro)*, v. 27, n. 2, pp. e13226, Jan. 2023. doi: <http://dx.doi.org/10.1590/s1517-707620220002.1326>.
- [42] MATEAB, S., ALBOZAHID, M., “Study the effect of adding MWCNTS on the hardness, impact strength, and structural properties of composite materials based on epoxy polymer”, *Egyptian Journal of Chemistry*, v. 65, n. 3, pp. 147–152, 2022. <http://dx.doi.org/10.21608/EJCHEM.2021.88640.4262>.
- [43] WANG, G., LIU, L., ZHANG, Z., “Interface mechanics in carbon nanomaterials-based nanocomposites”, *Composites. Part A, Applied Science and Manufacturing*, v. 141, pp. 106212, Feb. 2021. doi: <http://dx.doi.org/10.1016/j.compositesa.2020.106212>.
- [44] MENSAH, B., GUPTA, K.C., KIM, H., *et al.*, “Graphene-reinforced elastomeric nanocomposites: a review”, *Polymer Testing*, v. 68, pp. 160–184, Jul. 2018. doi: <http://dx.doi.org/10.1016/j.polymertesting.2018.04.009>.
- [45] SHEN, J., LI, X., LI, P., *et al.*, “Exploring thermodynamic and structural properties of carbon nanotube/thermoplastic polyurethane nanocomposites from atomistic molecular dynamics simulations”, *RSC Advances*, v. 13, n. 30, pp. 21080–21087, 2023. doi: <http://dx.doi.org/10.1039/D3RA03000H>. PubMed PMID: 37448641.
- [46] LI, L., XU, L., DING, W., *et al.*, “Molecular-engineered hybrid carbon nanofillers for thermoplastic polyurethane nanocomposites with high mechanical strength and toughness”, *Composites. Part B, Engineering*, v. 177, pp. 107381, Nov. 2019. doi: <http://dx.doi.org/10.1016/j.compositesb.2019.107381>.
- [47] DOWNES, R.D., HAO, A., PARK, J.G., *et al.*, “Geometrically constrained self-assembly and crystal packing of flattened and aligned carbon nanotubes”, *Carbon*, v. 93, pp. 953–966, Nov. 2015. doi: <http://dx.doi.org/10.1016/j.carbon.2015.06.012>.
- [48] WANG, S., GAO, E., XU, Z., “Interfacial failure boosts mechanical energy dissipation in carbon nanotube films under ballistic impact”, *Carbon*, v. 146, pp. 139–146, May. 2019. doi: <http://dx.doi.org/10.1016/j.carbon.2019.01.110>.
- [49] NAGHIZADEH, Z., FAEZIPOUR, M., HOSSEIN POL, M., *et al.*, “High velocity impact response of carbon nanotubes-reinforced composite sandwich panels”, *The Journal of Sandwich Structures & Materials*, v. 22, n. 2, pp. 303–324, Feb. 2020. doi: <http://dx.doi.org/10.1177/1099636217740816>.
- [50] JOY, J., GEORGE, E., THOMAS, S., *et al.*, “Effect of filler loading on polymer chain confinement and thermomechanical properties of epoxy/boron nitride (h-BN) nanocomposites”, *New Journal of Chemistry*, v. 44, n. 11, pp. 4494–4503, Mar. 2020. doi: <http://dx.doi.org/10.1039/C9NJ05834F>.
- [51] NAKAGAWA, S., MARUBAYASHI, H., NOJIMA, S., “Crystallization of polymer chains confined in nanodomains”, *European Polymer Journal*, v. 70, pp. 262–275, Sep. 2015. doi: <http://dx.doi.org/10.1016/j.eurpolymj.2015.07.018>.
- [52] BASHPA P, BIJUDAS K, FRANCIS T, “Enhanced dielectric and thermal properties of thermoplastic polyurethane/multi-walled carbon nanotube composites”, *Materials Today: Proceedings*, v. 51, n. Pt. 8, pp. 2254–2259, Jan. 2022. doi: <https://doi.org/10.1016/j.matpr.2021.11.393>.

- [53] WANG, X., XUE, R., LI, M., *et al.*, “Strain and stress sensing properties of the MWCNT/TPU nanofiber film”, *Surfaces and Interfaces*, v. 32, pp. 102132, Aug. 2022. doi: <http://dx.doi.org/10.1016/j.surfin.2022.102132>.
- [54] GAHLOUT, P., CHOUDHARY, V., “EMI shielding response of polypyrrole-MWCNT/polyurethane composites”, *Synthetic Metals*, v. 266, pp. 116414, Aug. 2020. doi: <http://dx.doi.org/10.1016/j.synthmet.2020.116414>.
- [55] LEE, H.D., YOO, B.M., LEE, T.H., *et al.*, “Defect-free surface modification methods for solubility-tunable carbon nanotubes”, *Journal of Colloid and Interface Science*, v. 509, pp. 307–317, Jan. 2018. doi: <http://dx.doi.org/10.1016/j.jcis.2017.09.037>. PubMed PMID: 28918373.
- [56] SINGH, O., BEHERA, B.K., “Review: a developmental perspective on protective helmets”, *Journal of Materials Science*, v. 58, n. 15, pp. 6444–6473, Apr. 2023. doi: <http://dx.doi.org/10.1007/s10853-023-08441-3>.
- [57] OZTURK, U.E., ANLAS, G., “Finite element analysis of expanded polystyrene foam under multiple compressive loading and unloading”, *Materials & Design*, v. 32, n. 2, pp. 773–780, Feb. 2011. doi: <http://dx.doi.org/10.1016/j.matdes.2010.07.025>.
- [58] WU, F., QIANG, S., ZHANG, X., *et al.*, “The rising of flexible and elastic ceramic fiber materials: fundamental concept, design principle, and toughening mechanism”, *Advanced Functional Materials*, v. 32, n. 45, pp. 2207130, 2022. doi: <http://dx.doi.org/10.1002/adfm.202207130>.